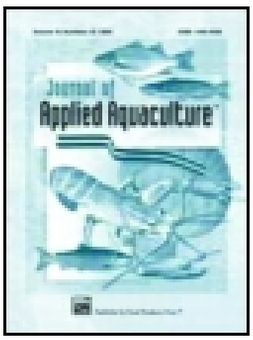

Journal of Applied Aquaculture

ISSN: 1045-4438 (Print) 1545-0805 (Online) Journal homepage: http://www.tandfonline.com/loi/wjaa20

A model to assess trade-offs between environmental impact and profitability of offshore salmon farms: A case study on Chile

Kelsey I. Jacobsen, Willow J. Battista, Lindsey M. Kaplan, Jennifer L. Price Tack, Marisa D. Villarreal & Cristopher Costello

To cite this article: Kelsey I. Jacobsen, Willow J. Battista, Lindsey M. Kaplan, Jennifer L. Price Tack, Marisa D. Villarreal & Cristopher Costello (2016): A model to assess trade-offs between environmental impact and profitability of offshore salmon farms: A case study on Chile, Journal of Applied Aquaculture, DOI: 10.1080/10454438.2016.1175831

To link to this article: http://dx.doi.org/10.1080/10454438.2016.1175831

Published online: 05 Jul 2016.

JOURNAL OF APPLIED AQUACULTURE
http://dx.doi.org/10.1080/10454438.2016.1175831

Taylor & Francis
Taylor & Francis Group

A model to assess trade-offs between environmental impact and profitability of offshore salmon farms: A case study on Chile

Kelsey I. Jacobsen[a], Willow J. Battista[a], Lindsey M. Kaplan[a], Jennifer L. Price Tack[a,b], Marisa D. Villarreal[a], and Cristopher Costello[a]

[a]Bren School of Environmental Science and Management, University of California, Santa Barbara, Santa Barbara, California, USA; [b]School of Forestry and Wildlife Sciences, Auburn University, Auburn, Alabama, USA

ABSTRACT

In recent decades, aquaculture has emerged as a viable method to help supply the growing global demand for seafood; however, expansion of the industry comes with potential negative impacts. Regulatory decisions governing aspects like aquaculture farming practices and farm siting inherently lead to trade-offs between profitability and the health of the surrounding environment through impacts including pollution, disease, and disturbance from escaped fish. Efficiently and sustainably scaling up aquaculture will require the development of methods for explicitly examining the trade-offs among these impacts and socioeconomic objectives. We developed a model to assess these trade-offs and illustrate the approach with a case study of salmon aquaculture in southern Chile. In the case study we found evidence that all 21 farms with approved permits may be underperforming on both profitability and the protection of ecosystem health. Our model suggests that explicit evaluation of trade-offs can illuminate the potential for improvements on multiple outcomes simultaneously.

KEYWORDS

Aquaculture; bioeconomic model; Chile; coastal industries; farmed salmon; trade-off analysis

Introduction

There are numerous models that predict the interactions between salmon aquaculture operations and their associated biological and economic systems (e.g., Cacho 1997; Mccausland et al. 2006; Nobre et al. 2009; Sylvia et al. 1996); however, such bioeconomic models have traditionally aimed to optimize production, ignoring aquaculture's effects on ecosystem services and socioeconomic impacts such as through worker welfare and effects on other industries (Pomeroy et al. 2008). The bioeconomic model developed by Mccausland et al. (2006) provides a production function that takes into account aquaculture's interactions with labor markets, regulations, traditional fishing, and the physical marine environment. However, their model focuses on the implications of increased regulation on employment and fish production, and it focuses on

CONTACT Jennifer L. Price Tack jlprice22@gmail.com School of Forestry and Wildlife Sciences, Auburn University, 602 Duncan Drive, Auburn, AL 36849, USA.

the industry as a whole instead of on individual concessions. In addition, the McCausland model addresses environmental impacts with respect to their effects on farmed salmon and the physical environment but does not translate these changes to impacts on the surrounding wild biota. Finally, the model does not account for potential catastrophic events like virus outbreaks. There are currently no bioeconomic models of offshore aquaculture that explicitly explore the trade-offs between environmental and socioeconomic interests and incorporate potential costs of disease outbreaks and labor law violations. This research gap is particularly important for regions with impending expansion of the offshore aquaculture industry, such as the Magallanes region of southern Chile.

Numerous studies have demonstrated that aquaculture activities in Chile result in a variety of environmental (Barton 1997; Buschmann et al. 1996, 2006; Soto et al. 2001) and socioeconomic (Barrett et al., 2002; Fløysand et al. 2010; Pitchon 2011) trade-offs. Some of these studies highlight the results of the implicit trade-off that was made in Chile between aquaculture profitability and health of the coastal marine environment, which led to the near collapse of that region's salmon farming industry and widespread degradation of the coastal environment (Nash et al. 2005; Ocean Conservancy 2011). These studies provide informative descriptions of impacts that the industry has caused, but they do not offer mechanisms for avoiding or mitigating the negative impacts of offshore aquaculture in the future. By providing a scientific basis to help guide management decisions, the model presented here can enable decision makers to shift from a trial-and-error approach to a scientifically informed, proactive approach to offshore aquaculture management.

Methods

We constructed a bioeconomic model to predict the impacts of certain salmon farming practices, given certain biophysical conditions, on various outcomes of socioeconomic and environmental interest. In this article, we focus on two key outcomes: Concession Profit (CP) and Ecosystem Health (EH). These two outcomes were chosen due to their high level of stakeholder interest and their tendency to lead to perceived trade-offs. Although these two outcomes are the focus of this analysis, our model is also capable of analyzing other outcomes, including risk of disease or parasite outbreak, cost of regulatory violations such as labor laws, and economic impacts on the artisanal fishing and tourism industries (Battista et al. 2012).

Our model generates results at the scale of a single salmon aquaculture concession for one production cycle of 12–18 months, where a production cycle begins when the salmon smolt are transported to offshore pens and ends when they are harvested as adults.

Focusing on the outcomes of EH and CP, we first identified a selection of inputs, comprising farming practices and biophysical conditions, that affect those outcomes (Table 1). To quantify the effects on EH and CP of varying the input values, we created six submodels that can be parameterized for a particular part of the world. These submodels are: Nutrients, Chemicals, Escapes, Aquaculture Concession Revenue and Costs, Risk Cost of Regulatory Violations, and Risk Cost of ISA Transmission. For the Cost of Regulatory Violations submodel, we focused on labor regulations, as this is an issue of concern in Chile and other salmon farming regions. The submodels are composed of mathematical relationships drawn from scientific literature and parameter values from scientific literature, primary sources, and authors' estimates.

It is worth noting that the model does not measure or account for cumulative effects over time, nor does it account for the cumulative effects of multiple concessions operating in the same area, as modeling the mathematical cause-and-effect relationships of outputs and inputs over time was outside the scope of our approach. However, understanding the cumulative effects of aquaculture operations over time and space would be beneficial in making management decisions. Future efforts to adapt the model to measure and account for cumulative impacts could increase its utility as a management tool.

Figure 1 provides a conceptual diagram of the model and its outputs. The lines connecting the various components of the model indicate where there is a mathematical connection between each input and outcome by way of the six submodels and their respective outputs. Each submodel is described in the following section; further details can be found in (Battista et al. 2012).

Ecosystem health

Nutrients

This submodel was constructed to predict the impacts on native biota of nutrients flowing out of salmon farms, which primarily originate from salmon feces and uneaten food. Due to the lack of data on the complex biogeochemical processes underlying nutrient limitation in many salmon farming regions, and findings of previous studies that indicate that nitrogen

Table 1. Complete list of modeled inputs, each describing one salmon farming concession.

Input	Biophysical Condition (BC) or Farming Practice (FP)
Number of net pens	FP
Current speed	BC
Water depth	BC
Cycle length	FP
Starting number of smolt	FP
Number of chemical treatments	FP
Equipment quality	FP
Number of hours violations	FP
Number of wage violations	FP

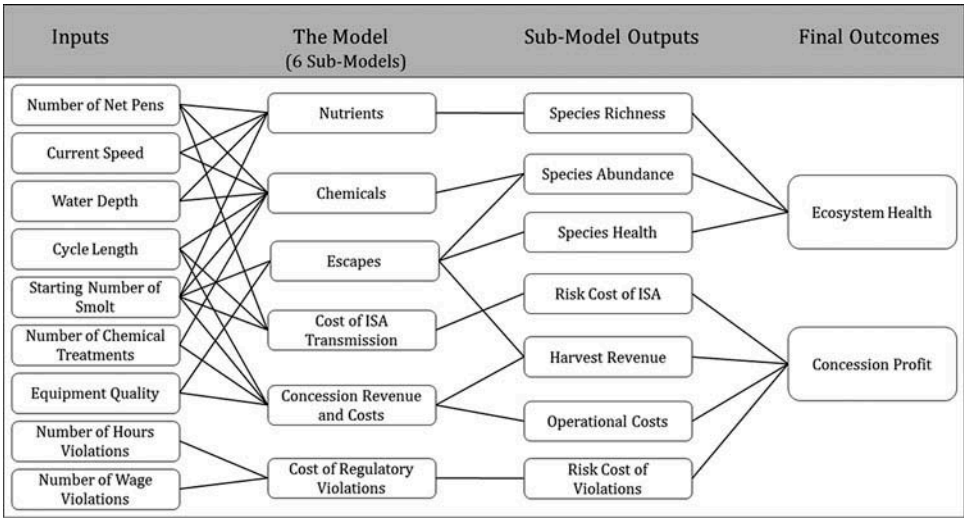

Figure 1. Conceptual diagram of inputs' links to outcomes in the model. Lines indicate mathematical relationships between the model's inputs and outcomes; they do not represent all conceptual or ecological relationships.

is often the limiting nutrient in coastal marine ecosystems (e.g., Howarth 1988; Rabalais 2002), we assumed from the outset that nitrogen (N) is the limiting nutrient in the waters surrounding salmon farms. Accordingly, this submodel is built upon a mathematical relationship from Gao et al. (2005) that describes the change in benthic species richness based on the amount of N loading in a marine system:

$$H' = 0.44 + \frac{3.79}{N}$$

where *H'* represents the Shannon Index (Shannon 1948), which uses measures of species richness and evenness to estimate species diversity (Azavedo et al. 2015); for brevity, we simply refer to the outcome of this submodel as species richness. *N* represents Total Kjeldahl Nitrogen, which is assumed to constitute all N loading from salmon food and feces. Although some nitrogen may leach into the water, we assume that all nitrogen contained in food and feces reaches the seafloor. Because the species richness of specific salmon farming locations is likely to be unknown, we constructed this submodel to predict the percent change in species richness by calculating the point elasticity of Gao et al.'s (2005) model at the average N concentration reported by that study over the course of nutrient loading from salmon farms. The elasticity indicates a 2.8% decrease in *H'* with every 1% increase in N.

Next, we estimated the total mass of N entering the marine environment from one farm over one harvest cycle:

$$N_{total} = E \times F \times C_{food} \times Y \times K + C_{feces} \times (1 - F) \times Y \times K$$

where N_{total} represents the total mass of nitrogen entering the marine environment from one farm over one harvest cycle. E = the percent of consumed feed that is excreted in feces; F = the percent of applied feed that is consumed by the salmon; C_{food} = the N content of salmon feed by weight; Y = the economic food conversion ratio; C_{feces} = the percent N content by weight in salmon feces; and K = the salmon production expected from one farm during one harvest cycle, as predicted from the results of the Aquaculture Revenue and Costs submodel.

We incorporated the spatial effects of particle movement to predict the farthest distance that N travels in the direction of the prevailing current before reaching the seafloor (d). This dispersal model is based on an equation from Silvert and Sowles (1996):

$$d = \frac{W \times D}{(s_{feces} + s_{feed})/2}$$

where W is current speed, D is water depth, and s is settling speed.

This distance was used to determine the "impact area," an elliptical area with major axis equal to d, within which all N originating from a salmon farm is deposited onto the seafloor. The farthest distance that particles travel perpendicular to the current (equal to ½ of the ellipse's minor axis), e, was calculated using a modified version of the equation used to calculate d:

$$g = \frac{\ln(W) \times D}{(s_{feed} + s_{feces})/2}$$

N deposition was assumed to follow a normal distribution, with decreasing N loading at increasing distances from the farm (Black et al. 2008). To model this pattern, the impact area was represented by concentric elliptical rings radiating from the farm and separated by 5 m on the major axis. For mathematical purposes, the farm is assumed to be at the center of the ellipse, although in reality it is located at one end of the ellipse (see Figure 2). We used a cumulative distribution function (mean = 0, $sd = 1/6d$) to estimate the proportion of the N effluent that falls within each elliptical ring. We then multiplied that proportion by N to find the mass of N falling within each ring.

Due to lack of data describing the seafloor composition at farming sites, we assumed that the seafloor is homogenous, so N will incorporate into all affected seafloor substrates equally. We used the area and volume of each ring, the background N density, and the density of the dominant sediment of sand (Montiel et al. 2011) to translate these masses of N into densities. The background N densities (Farías 2003; Gao et al. 2005) and total densities after a cycle of salmon farming were then used to calculate the fractional change in

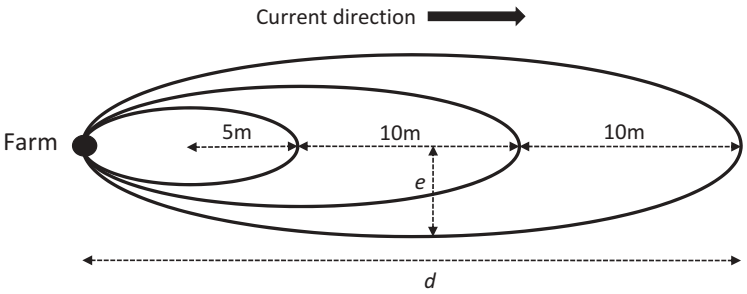

Figure 2. Diagram of particle dispersal from a hypothetical salmon farm.

N density experienced by each ring. Those values were in turn used to calculate the fractional change in species richness in each ring based on the elasticity of −2.8. We added the (negative) fractional change in species richness in each ring to 1 to determine the fraction of species richness remaining in each ring after one harvest cycle.

We calculated each concentric elliptical ring's contribution to the overall species richness remaining within the entire impact area and summed those weighted contributions to find the fraction of species richness remaining in the whole impact area. We standardized the submodel result by reporting the size of the impact area and the fraction of species richness remaining within 100 m of the farm in the direction of the current. Standardizing in this way allows for comparison of impacts among different-sized impact areas and with the results of the Chemicals submodel.

Chemicals

Salmon aquaculture utilizes a wide variety of chemicals, including antibiotics, parasiticides, antifoulants, anaesthetics, and disinfectants. The use of these chemicals worldwide is highly variable depending on existing regulations, availability, environmental conditions, and farm-specific needs. For this study, we chose to model the impacts of two chemicals that are used extensively in salmon aquaculture. We selected a common parasiticide, emamectin benzoate (SLICE®), and copper-based antifouling paint (Burridge et al. 2010). Despite the environmental concerns raised by antibiotic use, we elected to exclude antibiotics from our model because such impacts (i.e., the development of antibiotic resistance) are highly complex and likely take years to be detected.

Like nutrients, copper and SLICE accumulate in the sediments under salmon farms. Copper-based antifouling paints are commonly used to coat the surfaces of net pen structures to deter the growth of barnacles and other fouling organisms. Studies have demonstrated that copper concentrations in benthic sediments surrounding farm sites can exceed toxic thresholds and result in a multitude of impacts on benthic species (Burridge et al. 2010).

SLICE is a chemical added to salmon feed to destroy parasitic sea lice, and studies have documented negative impacts of SLICE on crustaceans (Mayor et al. 2008; Veldhoen et al. 2012).

We model the impacts of copper and SLICE on benthic invertebrates because these organisms are highly susceptible to contaminants in benthic sediments surrounding farm sites (Burridge et al. 2010; Mayor et al. 2008). To quantify the impact of these chemicals on benthic organisms, we first calculated the amounts of copper and SLICE that originate from a salmon farm and are deposited in marine sediments over the course of one harvest cycle:

$$SLICE: {}^{Total\ SLICE\ Input = \varpi \times S \times \Psi \times \Lambda}$$

where ϖ = the average weight of one salmon over the cycle length, N = total number of fish per farm, Ψ = dosage of SLICE, and Λ = number of treatments per cycle.

$$Copper: {}^{Total\ Copper\ Input = \iota \times \Gamma \times \kappa \times \eta \times \Upsilon_n}$$

where ι = leaching rate, Γ = number of months per cycle, κ = number of days in a month, Υ_n = painted surface area of one net, and η = number of net pens per farm. To quantify the painted surface area of a given net, Υ_n, we estimated:

$$\Upsilon_n = (\varsigma - \varrho) \times \upsilon$$

where ς = the surface area of the outside of a box representing a rectangular net, ϱ = the area of the top of the box, and υ = the fraction of the box surface that is a painted with copper.

Deposition of SLICE and copper onto the seafloor. We modeled deposition of SLICE and copper onto the benthos with the same method used in the nutrients submodel. Because SLICE is a component of salmon feed, we averaged the settling speed of feed and feces to determine the maximum distance that SLICE travels from a salmon farm. No settling speed was available in the literature for copper, so we assumed a settling speed of 4 cm/s based on that of feces (Chen et al. 2003; Tironi et al. 2010) due to the small size of leached copper particles. We assumed that the distance calculated using the average settling speed, current speed, and depth is the maximum distance traveled by food and feces from the farm. Like the Nutrients submodel, we assumed a normal distribution (mean = 0, $sd = 1/6d$) of particle deposition into concentric elliptical rings emanating from the salmon farm (Chen et al. 2003; Tironi et al. 2010). The maximum distance that a particle travels in a direction perpendicular to the current was calculated in the same way as in the Nutrients submodel. We then used the total amount of chemical input to calculate the concentration of copper and SLICE deposited within each ellipse.

Effects of SLICE and copper on benthic species. Using the modeled concentrations of copper and SLICE within the concentric rings of the impact area after one harvest cycle, we calculated the fraction of benthic invertebrates that die in each ring due to SLICE or copper, based on a study by Mayor et al. (2008) on polychaetes and crustaceans:

$$\text{Effects of SLICE:}$$

$$\textit{Fraction Mortality of Polychaetes} = 1(1 + e^{1.15-0.002\times[SLICE]})^{-1}$$

$$\textit{Fraction Mortality of Crustaceans} = 1\left(1 + e^{1.22-0.002\times[SLICE]}\right)^{-1}$$

$$\text{Effects of Copper:}$$

$$\textit{Fraction Mortality of Polychaetes} = 1\left(1 + e^{3.3-3.3541\times10^{-5}\times[Copper]}\right)^{-1}$$

$$\textit{Fraction Mortality of Crustaceans} = 1\left(1 + e^{1.5-9.866\times10^{-6}\times[Copper]}\right)^{-1}$$

where *[SLICE]* and *[Copper]* = the concentration of SLICE and copper respectively in the sediments.

We then calculated overall mortality within the ellipse bounded by a dispersal distance of 100 m for both copper and SLICE. We subtracted the resulting fractional mortality from 1 to find the fraction of each benthic species remaining in the impact area after one harvest cycle and then averaged the effects of SLICE and copper on crustaceans and polychaetes. We take an average of this model and the Nutrient submodel to give an index of species abundance.

Escaped salmon

We constructed a submodel to predict the impacts of escaped farmed salmon on wild species through predation, competition, and spread of disease and parasites. We chose to model these impacts of escaped salmon because they are among the most significant concerns associated with salmon farming on a large scale (Buschmann et al. 2009; Naylor et al. 2005). Escaped salmon compete with native species for food and other resources and may prey on some native species as well (Buschmann et al. 2009). These impacts can be exacerbated if the local environmental conditions are favorable for the farmed salmon's long-term survival and establishment in the new ecosystem (Naylor et al. 2005); however, it is unlikely that escaped Atlantic salmon are able to establish and persist in southern Chile (Soto et al. 2001). Furthermore, escaped salmon can facilitate the spread of diseases and parasites from salmon pens to wild organisms (Buschmann et al. 2009; Jensen et al. 2010; Naylor et al. 2005; Ocean Conservancy 2011; World Wildlife Federation [WFF] 2009).

In addition to impacts on wild organisms, the Escapes submodel quantifies financial losses to the concession due to escaped salmon as well as the operational costs associated with several net pen technologies that perform at varying levels on preventing salmon escapes (see the Appendix).

Equipment quality. To model the effect of escaped salmon on native species, we assumed that the percent of smolt that escape during each cycle is dependent on the quality of the net pen technology, with poorer quality technologies allowing more escapes. We defined four distinct Technology Classes, ranging in quality from dilapidated cloth nets to potential new copper cage technology, with escape rates of 30%, 20%, 5%, and 0%, respectively, based on literature and expert interviews (Jensen, pers. comm., 2012; Molina, pers. commun., 2012; Naylor et al. 2005).

Predation and competition. To model the predation and competition pressures of escaped salmon on wild species, we first used the Lotka-Volterra equations, adjusted for density-dependent growth, to describe the interactions between native predator and prey species in the absence of escaped salmon. We then added the number of escaped salmon as an additional predator-level pressure and examined the effects on three trophic levels: predator-level finfish, prey-level finfish, and cetaceans.

We manipulated these equations (see the Appendix) to find the fractional change in the numbers of native individuals remaining with and without pressure from escaped salmon and found these relationships to be linear. We then used records from a number of large-scale salmon escape events (Buschmann et al. 2006; Jensen, pers. comm., 2012; Soto et al. 2001; WWF 2009), combined with observations of percent reductions of native species in corresponding locations and times (Soto et al. 2006), to extrapolate that an escape event of approximately 50,000 salmon would result in a 50% reduction in wild predator and prey populations. We assumed that 100,000 escapes in one cycle would be required to reduce the population of cetaceans by 50% because competition pressure from salmon on cetaceans is lower than on finfish. The following equations describe these relationships:

$$FractionalChangePredator = 1 - \left(\left(\frac{0.5}{50,000}\right) \times [predicted\#escapes]\right)$$

$$FractionalChangePrey = 1 - \left(\left(\frac{0.5}{50,000}\right) \times [predicted\#escapes]\right)$$

and

$$FractionalChangeCetaceans = 1 - \left(\left(\frac{0.5}{50,000}\right) \times [predicted\#escapes]\right)$$

where the predicted number of escapes is calculated based on the percent determined by the Technology Class in use (see the Appendix).

Disease transmission. We based our model predicting the spread of disease and sea lice, both among farmed salmon and from farmed salmon to wild species, on equations detailed by Anderson and May (1979). We assumed that escapes are the only source of disease transfer to the native species and that no salmon or native species become immune or resistant to the disease. Furthermore, we assumed that the disease and sea lice only transfer between individuals via direct contact, and we thus did not attempt to model virus dilution in the water column, which would be dependent on the specific hydrology of a given region. Equations for disease transfer within pens are as follows, modified from Anderson and May (1979):

$$\frac{d\mathrm{H}}{dt} = \Theta - \mathrm{HM} - \mu\mathrm{H}\sigma - \mathrm{H}\varepsilon$$

and

$$\frac{d\sigma}{dt} = \mu\mathrm{H}\sigma - (\sigma(\mathrm{M} + \nu)) - \sigma\varepsilon$$

where H = number of healthy individuals, σ = number of diseased individuals, t = time in months, Θ = population growth of healthy animals, M = natural mortality rate for healthy individuals, μ = disease (or sea lice) transmission coefficient, ν = mortality rate due to the disease (or sea lice), and ε = percent of individuals that escape (based on Technology Class).

To transform these equations to predict the spread of disease from escaped salmon to native species, we added a term, Z, as an additional disease source in the system. Z represents the number of escapes each month that are infected with the disease and is calculated by multiplying the number of diseased salmon in a concession by the Technology Class' escape rate:

$$\frac{d\mathrm{H}}{dt} = \Theta - \mathrm{HM} - \mu\mathrm{H}(\sigma + \mathrm{Z})$$

and

$$\frac{d\mu}{dt} = \mu\mathrm{H}(\sigma + \mathrm{Z}) - (\sigma(\mathrm{M} + \nu))$$

We based disease mortality rates and transmission coefficients on infectious pancreatic necrosis (IPN), a virus that has important implications for farmed salmon populations and can be transmitted to native species (Guy et al. 2006; Hnath 2002; McAllister 1983). We chose to model this virus instead of the better known ISA because unlike ISA, IPN can sometimes go undetected for

many months and may therefore not be addressed by managers before spreading throughout the farmed population and beyond. Our goal was to select a single virus that could represent "the spread of disease" more generally. The model could be parameterized with the specific characteristics of another disease of interest to users in a specific location if they are known. We based disease mortality rates and transmission coefficients on infectious pancreatic necrosis (IPN), a virus that has important implications for farmed salmon populations and can be transmitted to native species (Guy et al. 2006; Hnath 2002; McAllister 1983).

The spread of sea lice was modeled similarly to disease but with the following adjustments: (1) the equations were amended to incorporate salmon's contraction of sea lice from native species (see the Appendix for calculations), (2) mortality rates due to sea lice were assumed to be much lower than that of disease, and (3) the transmission coefficient for sea lice was assumed to be much higher. All parameter values can be found in Table A3 in the Appendix.

Finally, we calculated the fractional changes in the numbers of healthy individuals of native species in each trophic level at the end of one harvest cycle by dividing the number of healthy individuals remaining at the end of the cycle by the roughly estimated number of individuals present at the start of the cycle (see the Appendix). As with the predation and competition submodel, this model calculates fractional rather than absolute population changes, and the results are thus applicable to any spatial scale, making it possible to combine them with the results from the Nutrients and Chemicals submodels (see the following).

Throughout the Escapes submodel we model the fractional, rather than absolute, changes in numbers of individuals of wild species using a spatially independent model due to the high level of mobility of many impacted species. This submodel can thus be applied to any geographical area without the need to specify spatial parameters. For example, the starting number of healthy native individuals used for this case study was not known, and so instead we selected a value large enough to model changes over one aquaculture cycle without resulting in fractional numbers of healthy individuals. If data are available on the actual number of individuals of a given species in an area, this value could easily be substituted to make the model results more accurate to a specific site. In addition, measurement in terms of fractional change makes it possible to combine the results of the Escapes submodel with those of the Nutrients and Chemicals submodels (see the following Combining SubModel Outputs into Final Outcomes section).

One limitation of this submodel, as discussed regarding the exclusion of cumulative impacts in our model, is that we do not consider the additional effects of disease or sea lice from neighboring farms. Incorporating these

cumulative effects would be one way that this model could be improved upon in the future. We do, however, model the probability of one farm contracting the ISA virus from a neighboring infected farm based on stocking density and proximity in the ISA Transmission submodel (see the following ISA Transmission section).

Concession profit

Aquaculture revenue and costs

To determine the profit that a concession generates in one cycle, we modeled the revenue from selling one cycle's harvestable salmon as well as the costs of on-site operations, beginning when smolt are put into ocean net pens and ending after processing and transportation to wholesalers.

Harvest revenue. We calculated the number, individual weight, and value per weight of salmon that are available for harvest at the end of a cycle to determine the revenue from one concession from one harvest cycle. We based our model of biological growth on an equation developed by Asche and Bjorndal (2011), which reflects a relatively fast growth rate based on recent improvements to salmon farming methods:

$$w(t) = 5.72t^2 - 2.08t^3$$

where w = weight in kg and t = time in months.

We then factored in monetary losses due to escapes (calculated in the Escapes submodel) and mortality to find the percent of salmon that are lost over the course of a harvest cycle. We applied a decreasing mortality rate each month based on a step rate method described by Asche and Bjorndal (2011) and on research regarding expected mortality rates in Chilean (Guttormsen 2008) and Scottish (Soares et al. 2011) salmon farms.

We calculated the value, or revenue, of one cycle's harvest:

$$R(t) = 0.93b(t) \times 0.75p(t)$$

where R = total value in US dollars, t = time in months, b = total biomass in kg, and p = price in US dollars/kg of salmon.

Operational costs. We modeled the costs of producing one cycle's harvest at one concession using the variable costs calculated in the Chemicals, Risk Cost of Labor Violations (see following), and Escapes submodels:

$$\rho(t) = f(t) + q(t) + c(t) + m(t) + l(t) + i(t) + o(t)$$

where ρ = cost of production per kg harvested salmon, f = cost of feed per kg harvested salmon, q = cost of smolt per kg harvested salmon, c = cost of

chemicals per kg harvested salmon, m = cost of maintenance per kg harvested salmon, l = cost of labor per kg harvested salmon, i = interest and depreciation, and o = other operational costs. (See the Appendix for detailed calculations of the cost of feed, maintenance, chemicals, and labor.) Each of these variables is a function of the length of the harvest cycle.

We calculated the costs incurred before the salmon are sold on the commodity market *(a)*, which include processing, transportation, sales, and marketing, using a mathematical relationship established by Forster (1995):

$$a(t) = \left(\frac{\rho(t)}{1 - 0.38}\right) - \rho(t)$$

We then calculated the total cost of carrying out one cycle of aquaculture, *(C(t))*:

$$C(t) = h(t) \times b(t)$$

where h = the cost of harvest per kilogram of salmon, and

$$h(t) = \rho(t) + a(t) + L_{ISA} + v$$

where L_{ISA} = the expected cost of an ISA outbreak, and v = Risk Cost of Labor Violations.

Finally, we calculated Concession Profit from one harvest cycle:

$$P(t) = R(t) - C(t)$$

where P = profit, R = harvest revenue, and C = total cost of harvest.

ISA transmission

To model the probability and monetary impacts of ISA transmission between farms in the same concession, we first constructed a matrix of transmission scenarios. This matrix (Table 2) describes the probability of ISA transmission from a neighboring farm to a receiving farm during the span of 1 month, based on the starting state of both farms (infected/detected, infected/undetected, or uninfected). We assume that the detection of ISA occurs in the seventh month following the initial infection and that the monthly detection probability is 0.163 (see Table A2 in the Appendix). The monthly probability of initial infection is assumed to be 0.0008 (Scheel et al. 2007). We assume that a state change from uninfected or infected/undetected to infected/detected results in all salmon being slaughtered (Odebret, pers. comm., 2011). (See Table A2 for more assumptions used to build the probability matrix.)

We focus on scenarios in which, in month 1, the neighboring farm is infected and the receiving farm is uninfected, and in month 2 the receiving farm is infected. These specifications lead to three combinations of state changes of interest (highlighted in Table 2). Summing the probabilities of

Table 2. Probability matrix of ISA transmission scenarios with state changes of interest highlighted. Farm states for the two farms are described with positional values separated by commas, where the three positions (1,2,3) indicate the number of farms (0,1, or 2) that are (1) infected/detected, (2) infected/undetected, and (3) uninfected. For example, "1,1,0" indicates that one of the two farms is infected/detected, one farm is infected/undetected, and neither farm is uninfected. The bold values indicate situations in which one farm causes infection of a neighboring farm in the following month.

	Probability Matrix						
		Month 2					
Month 1		1,1,0	1,0,1	0,1,1	2,0,0	0,2,0	0,0,2
	1,1,0	0.000	0.837	0.163	0.000	0.000	0.000
	1,0,1	**0.000**	0.836	0.163	**0.001**	0.000	0.000
	0,1,1	0.000	**0.001**	0.000	0.000	0.000	0.999
	2,0,0	0.136	0.000	0.000	0.701	0.027	0.000
	0,2,0	0.000	0.000	0.000	0.000	0.000	1.000
	0,0,2	0.000	0.001	0.000	0.000	0.000	0.998

these three state changes and the baseline probability of infection from the natural environment yields an estimated probability of 0.0024 of the uninfected farm becoming infected with ISA in month 2.

We then utilize an existing model of ISA transm1ission developed by Scheel et al. (2007):

$$\lambda_{ji}(t) = \lambda_b(t)\exp\left(0.127n_j(t) + 0.102n_i(t)\right) \times \left[\exp\left(-0.415d\left(x_j, x_i\right)\right) + k_{ji}\exp(-2.013)\right]I_{ji}(t)$$

where $\lambda_{ji}(t)$ = the transmission rate from farm j to farm i, $\lambda_b(t)$ = the baseline transmission rate, $n_j(t)$ = the biomass at farm j, $n_i(t)$ = the biomass at farm i, and $d\left(x_j, x_i\right)$ = the distance between farms i and j. k_{ji} is a network indicator (equal to 1 if both farms are in the same concession, and 0 otherwise) and I_{ji} is a transmission indicator (equal to 1 if one farm is infected and the other is susceptible, and 0 otherwise) (Scheel et al. 2007). We calculated the proportional changes in ISA transmission rates using parameter estimates for biomass, distance, and local network terms calculated by Scheel et al. (2007) and assumed a 6-month delay in ISA detectability. The local network index refers to whether the farms are within the same concession, with transmission risk increasing when workers and boats travel between farms. We multiplied the proportional change in ISA transmission rates by the probability of the receiving farm becoming infected with ISA in month 2 (calculated previously) to estimate the probability of an ISA outbreak in the receiving farm.

To estimate the monetary impacts to a concession of ISA transmission, we calculated expected profit loss based on the probability of an ISA outbreak. We assume that once a farm becomes infected, there is a probability of 0.05 that the infection will spread throughout the entire farm, causing an outbreak. Therefore, we multiply the probability of ISA outbreak by 0.05 to determine the probability of an ISA outbreak given presence at a neighboring farm. We

assume that if an outbreak occurs and is detected, the fish are either slaughtered or harvested. If the outbreak occurs within the first 7 months of the cycle, the salmon are slaughtered and disposed of at a loss to the concession; if the outbreak occurs after the first 7 months, the salmon are harvested and sold. Therefore, the expected monetary loss (L_{ISA}) to a concession due to ISA is:

$$L_{ISA} = \Omega\delta(1 - O_m)$$

where O_m = the monthly operational cost, Ω = the probability of an ISA outbreak given infection in a neighboring farm, and δ = the number of months into the cycle at which the outbreak occurs. This value constitutes the submodel output Cost of ISA.

Risk cost of regulatory violations

There are numerous types of regulatory violations that a salmon farming facility can incur. These violations can be for environmental reasons such as using feed or chemicals in excess of the permitted amount, improper disposal of materials or refuse, or exceeding the approved number of salmon per pen. Violations can also pertain to the social dimension of salmon farming, such as labor standards. This submodel quantifies the potential and expected cost of violating labor laws, as these are some of the most common types of violations committed by salmon farms in Chile, where our case study was conducted. This submodel estimates the costs incurred by a concession due to fines for violating labor laws.

Labor law violations were categorized into wage violations and hours violations, where Wage Violations are defined as instances where any law regulating wage is violated, and Hours Violations are instances where any law regulating the legal number of working hours is violated.

The total potential cost of fines incurred for violating wage and hours violations cumulatively (TPC) was calculated using the formula:

$$TPC = (j \times r) \times +(\xi \times \Pi)$$

where j and u = the number of Wage Violations and the number of Hours Violations, respectively, during a production cycle. ξ and Π = the average fine amount in US dollars issued by the Chilean government for individual wage-based and hours-based labor violations, respectively.

The total expected cost of fines incurred for violating both wage and hours violations (TEC) was calculated by multiplying TPC by the probability of detection (θ). θ is assumed to be equal to the probability of inspection by regulatory officials, and it is assumed that the concession is in noncompliance with at least one wage or one hours law:

$$TEC = TPC \times \theta$$

where TPC represents the submodel outcome Risk Cost of Violations.

Combining submodel outputs into final outcomes

The final outcome of EH is an index comprised of the submodel outcomes Species Richness, Species Abundance, and Species Health. Despite the differing subjects with which each of these submodels deal, it is possible to combine these three values into a single index indicator of ecosystem health because each submodel was designed to generate a unit-less index, as opposed to a quantitative, concrete outcome value.

$$Ecosystem\ Health = Species\ Richness + Species\ Abundance + Species\ Health$$

The final outcome value for EH is a summation of the three species indices, where an individual index value of 1.0 for one of the three submodel indices indicates no change in EH. Consequently, a value of 3.0 indicates no change in EH after one cycle of salmon farming, while any value above or below 3 would indicate a change in the health of the ecosystem. While in reality there are likely to be interactions between the impacts of nutrient loading, chemical use, and salmon escapes on all three indices used to measure ecosystem health, summing the standardized submodel outputs provides a high-level indication of the direction of change in environmental health due to salmon farming.

The final outcome of CP was calculated by subtracting the submodel outputs Operational Costs, Cost of Violations, and Risk Cost of ISA from Harvest Revenue:

$$\begin{aligned} &Concession\ Profit \\ &= Harvest\ Revenue - (Operational\ Costs + Risk\ Cost\ of\ Violations \\ &+ Risk\ Cost\ of\ ISA) \end{aligned}$$

This outcome describes the total estimated profit that a concession would gain from a single production cycle operating under the specified input conditions.

Analyses

Trade-off analysis

To meet the need for an explicit approach for assessing the outcomes of different ocean management options, scientists have developed a method of trade-off analysis based on portfolio theory in economics (Polasky et al. 2008; White et al. 2012). Trade-off analysis allows managers to evaluate and visualize the outcomes of numerous management possibilities and identify those that are most efficient in terms of specified outcomes. This process enables managers to streamline the decision-making process by ruling out suboptimal plans and choose a plan that maximizes total benefits and prioritize outcomes of interest. Another benefit of the trade-off approach is that it allows analysis of outcomes that are measured in different units.

Figure 3 illustrates the trade-off analysis concept: Scenario 1 shows one possible management plan (plan A), with its point coordinates representing the resulting values of outcomes 1 and 2. Outcomes could be any measure of benefits relevant to the trade-off at hand, including revenue, jobs created, species protected, pollution mitigated, etc. Another management plan (B) might exist, which is preferable because it performs better than A on one or both outcomes (Scenario 2). A third plan (C; Scenario 3) might perform better than B on one outcome but worse on the other, signaling a trade-off that would require judgment about which outcome to prioritize in order to choose the preferred plan. Plans B and C create an "efficiency frontier" that delineates the outer bound—that is, the most efficient plans—among the three given plans. This stage of the trade-off analysis can be used in decision-making processes to identify the most efficient plans and rule out those that fall short of achieving maximum total benefits. It is possible, however, that other management plans exist that are even more efficient than those proposed (plan D; Scenario 4). Modeling can reveal such plans by assessing large numbers of hypothetical plans with different combinations of possible input values. In this way, trade-off analysis can not only evaluate the outcomes of current management actions but can also reveal possible superior plans that would lead to greater benefits for one or both outcomes.

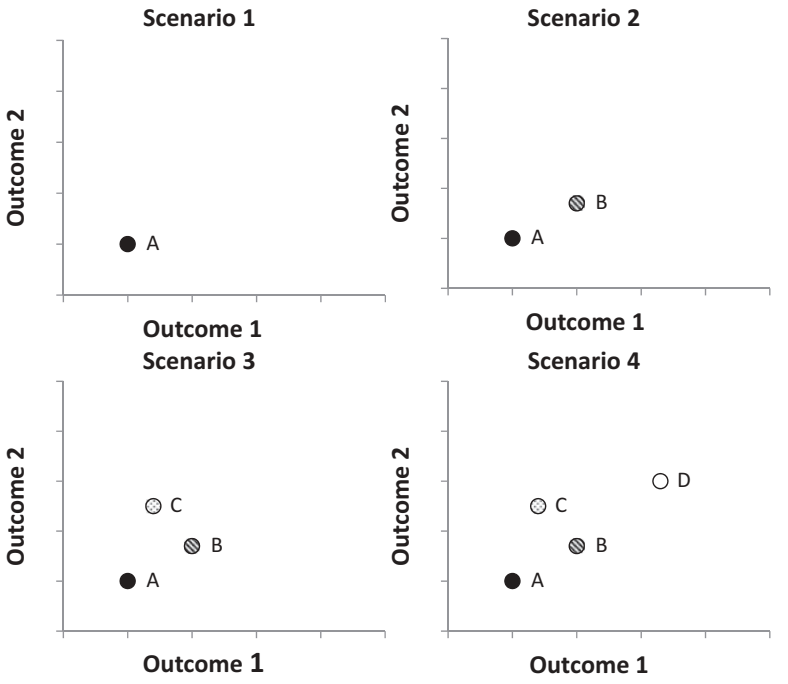

Figure 3. Plots of a generic trade-off analysis.

Case study

Trade-off analysis offers a promising tool for evaluating the effects of salmon aquaculture on socioeconomic and environmental outcomes, which can help guide offshore aquaculture management. To assess the trade-offs in an actual aquaculture scenario, we performed a trade-off analysis using our model, which we parameterized based on salmon aquaculture operations in southern Chile. This area is currently experiencing aquaculture growth and offers a relevant example of the conflicts between environmental and economic interests. In our case study, each point on the trade-off space represents one approved or hypothetical salmon farming concession based on its unique combination of input values. The concession's point coordinates represent the resulting outcome values of EH and CP. The model can be used to plot predicted outcome values for proposed concessions and to generate an efficiency frontier by evaluating outcomes for a large number of hypothetical concessions.

Since the 2007 collapse, the Chilean salmon farming industry has begun to rebuild and expand into the country's southernmost region, the Magallanes. However, there is currently no mechanism in Chilean legislation for evaluating and comparing the potential ecological and economic impacts of salmon aquaculture operations. During this period of expansion and new policy development, our model can serve as a valuable asset for managers by offering a mechanism by which to explicitly assess the trade-offs between environmental and economic impacts and guide management decisions.

Offshore salmon aquaculture in Chile is currently managed through a system of spatial allocations. Aquaculture may only be practiced within defined coastal areas identified by the government as Appropriate Areas for Aquaculture (AAAs). Within the AAAs are smaller areas—concessions—that can be leased from the government for the purposes of cultivating salmon. To obtain a lease for a salmon aquaculture concession, an aquaculture company must provide some specific information about its proposed operation, including biophysical conditions (e.g., depth of the sea floor and average current speed) and aquaculture practices (e.g., amount of feed used and the numbers of net pens, smolt, and workers required). This information is submitted to the Chilean government in Environmental Impact Assessment (EIA) documents; at the time of this model's development, 21 concessions had been approved by the Magallanes government.

Case study methods

To model the effects of salmon farming concessions in southern Chile, we parameterized our model with data specific to Chile wherever possible and used data from other parts of the world where Chile-specific data were not available (see Table A3). We determined input and parameter values based

on literature, the EIAs of the 21 approved concessions, and authors' estimates. Parameterizing the model with values from existing regulatory and planning documents helped to establish our model's relevancy, credibility, and alignment with the existing management systems in Chile.

We programmed our model in MATLAB such that each model run represents one possible management plan, that is, a combination of input values that can be selected by the aquaculturist (or required by the government). The resulting outcome values are those that can be expected after one harvest cycle under the management plan conditions. We ran the model once for each of the 21 approved concessions, using the input values given in their EIAs. We set parameter values to default values, which were collected from the literature or calculated as the average values reported in the concession EIAs. We plotted the results of these model runs to assess the trade-offs between their outcomes for EH and CP (Figure 4).

To evaluate a wide range of hypothetical concessions, we assembled ranges for each input value by gathering the minimum and maximum values from the concession EIAs. These ranges are assumed to represent the full scope of possible farming practices and biophysical conditions in the Magallanes' salmon aquaculture areas. We then ran the model many times, each with a unique combination of inputs. Inputs were varied across their ranges in the following manner: If the input's range was large and continuous (for example, Number of Starting Smolt ranged from 300,000 to 3,000,000), we selected the lowest value, the highest value, and a midpoint value to represent this input's range. If the input's range was small and discrete (for example, Cycle Length ranged from 12 to 18 months), we included every value in its range. This process resulted in approximately 61,000 model runs, each representing a unique hypothetical concession. The full suite of these runs gives estimates of the ranges of EH and CP that can be expected as a

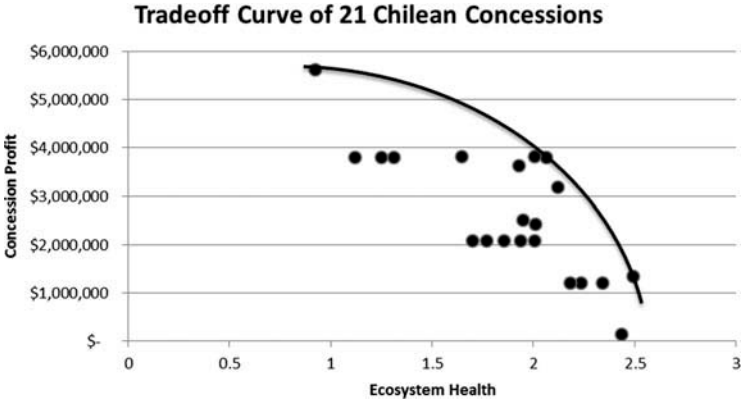

Figure 4. Ecosystem Health-Concession Profit trade-offs for the 21 approved salmon farming concessions for the Magallanes region of Chile.

result of one cycle of salmon aquaculture at one concession, assuming that input values fall within the determined ranges.

Plotting these results allows us to visualize the nature of the trade-off between EH and CP in the Magallanes, and identify the outcomes of and inputs leading to, the most efficient potential concessions. It is worth noting that although the two outcomes compared, EH and CP, are measured in different units, trade-off analysis is still valuable in that it illuminates the most efficient options in terms of both outcomes and illustrates the strength of the trade-offs between the two outcomes. If sufficient economic data were available to translate EH into value in dollars, managers could choose the options with the highest total dollar amount from both outcomes combined.

Results

Our analysis of the 21 approved concessions resulted in EH scores ranging from 0.9 to 2.5 and CP ranging from less than $135,000 to more than $5.6 million. The trade-off graph illustrating these results reveals a clear efficiency frontier (Figure 4) composed of three concessions: Concession A performs the best on CP (while compromising EH), Concession B performs the best on EH (while compromising CP), and Concession C strikes a more even balance between the two outcomes (see Table 3 for values). All of the other concessions fall inside of the efficiency frontier, indicating that they are suboptimal and could be altered to improve their scores on one or both outcomes.

The more than 61,000 model runs representing as many hypothetical concessions revealed an abundance of concessions that fall above the approved concessions' efficiency frontier and are therefore more efficient on EH and CP than even the most efficient approved concessions (Figure 5). These hypothetical conces-

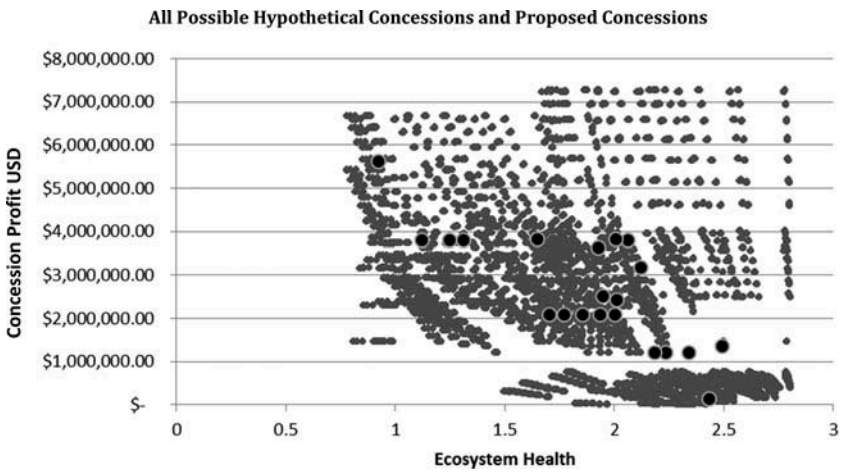

Figure 5. Ecosystem Health-Concession Profit trade-offs for proposed (black dots) and hypothetical (gray dots) concessions.

sions form a new efficiency frontier that represents the most efficient potential concessions. The shape of this efficiency frontier indicates that the trade-off between EH and CP can be very weak and that there are many hypothetical concessions that achieve high values for both EH and CP (i.e., the points near the outer apex of the frontier).

Discussion

Approved and hypothetical concession trade-offs

Our results demonstrate that there are many hypothetical concessions that fall well above all of the 21 approved Magallanes concessions on the trade-off space. Therefore, each of the approved concessions falling below the new efficiency frontier could be improved to result in higher scores on one or both outcomes. For example, managers of Concession A, which scored the highest of the 21 approved concessions on CP, could increase the Number of Net Pens, increase the Cycle Length, or upgrade Equipment Quality to result in higher scores for both CP and EH. Concession B, which scored highest in EH, could increase scores for both outcomes by increasing the Number of Net Pens, upgrading Equipment Quality, and increasing Stocking Density.

The model as a decision support mechanism

Our model enables the evaluation and visualization of the outcomes of a variety of salmon aquaculture concessions, which can be used to guide decisions regarding the selection of proposed concessions toward those that are the most efficient. However, our results do not indicate which of the efficient concessions are preferable. For example, our analyses do not reveal whether an efficient concession that scores high on EH and low on CP is better or worse than one that scores low on EH and high on CP; judgment is necessary for choosing the most appropriate concessions based on stakeholder priorities and objectives.

In addition to providing decision support for managers to select from proposed concessions, our model can be used to identify possible improvements to existing or proposed concessions that will lead to higher outcome scores. Stakeholders can adjust farming practices or siting decisions (or regulations governing them) to achieve outcomes that satisfy their priorities and objectives. The model can also be used to identify the farming practices and siting decisions that have the greatest effect on the outcome values, meaning that small modifications can lead to proportionally large changes in outcomes (see Battista et al. 2012 for an example of these calculations).

A counterintuitive implication of our results is the finding that concessions are not being managed in a way that maximizes profits; however, it is

our assertion that managers simply do not have access to all of the information necessary to make the most-informed decisions regarding farming practices. Our model offers a mechanism for managers and aquaculturists to identify areas for improvement.

In this article, we have highlighted the trade-off between EH and CP, but there are many other important relationships between outcomes of interest that represent the concerns of various industries and stakeholders; those trade-offs could be evaluated through an analysis similar to that which this study describes.

Conclusions

The global aquaculture industry is growing rapidly, and analyses like ours will be crucial for predicting its environmental and socioeconomic impacts and identifying efficient management options. Our model and trade-off analysis framework enable managers to select from the most efficient concessions, thereby maximizing overall benefits and avoiding the pitfalls of trial-and-error management that were exemplified by Chile's recent ISA crisis. While our model offers a framework for assessing trade-offs and managing aquaculture operations in diverse regions of the world, it should be seen as a first iteration of this analytical approach; improvements to the robustness and accuracy of the model may be explored in any future application of the model. There are some notable caveats with regards to the model's capabilities. First, as previously stated, our model predicts the effects of a single cycle of aquaculture. This limitation likely leads to underestimated levels of some environmental impacts that can have nonlinear cumulative effects over time, like through chemical and nutrient pollution. Similarly, our model does not take into account the cumulative effects of multiple concessions operating in the same area. Pollution resulting from farms that are close together, or in areas of higher current speeds or water depth, may result in overlapping impact areas that could lead to compounded ecosystem effects.

Furthermore, the shallow depths and slow current speeds associated with the most-efficient concessions highlights a trade-off inherent in our model between the size of the area affected by aquaculture pollution and the concentration of ecosystem effects. Shallower depths and slower currents result in more severe ecosystem effects, but these effects are concentrated in smaller areas. By reporting fractional changes in EH over an area of standard size, our model favors concessions that result in effects concentrated in small areas. However, there may be a feedback loop in small areas of acute impacts such that high levels of pollution jeopardize the health of the farmed salmon. Our model does not capture this relationship.

Building from the initial results of our model applied to the Chile case study, one potential area for future research would be to determine which of the EH components in reality play stronger roles in overall EH. Identifying

which components are more or less impactful could help to direct future management decisions and minimize the trade-offs between profit and environmental impacts.

Finally, while it offers a valuable framework and approach for aquaculture managers, aquaculture practitioners, and environmentalists, our model's predictions are limited by the factors that fall outside the scope of the model, which include genetic pollution of wild salmon and the exploitation of wild fish for use in farmed salmon feed. As with all mathematical models, the reliability of our results depends on the availability and quality of data on which it relies. We constructed and parameterized the model using data from existing regulatory planning documents to ensure the model's relevance and application to aquaculture management and to ground the model with real-world values. However, data were not available for all parameters or input values, and this likely reduces the accuracy of some of the calculations in the case study. Our model can, however, be parameterized with more accurate data as they become available and can be used as a framework on which to build additional submodels to represent additional aquaculture impacts. Furthermore, ground truthing the model's results with real-world data from farms that are in operation could test the model's accuracy and help legitimize its use for managers, regulators, practitioners, and more.

Concurrent with the expansion of aquaculture, there are a growing number of uses that compete for ocean space. Spatial trade-offs will therefore be important for coastal planners considering the development of aquaculture in the context of other offshore industries and uses. Our model can be implemented as a framework to predict the financial and environmental impacts of aquaculture, which can be weighed against the impacts of other coastal uses that compete for limited ocean space and resources. In addition, our model can be parameterized to describe many parts of the world where aquaculture is developing, thereby providing an adaptable approach for supporting sustainable aquaculture development. Models like ours will be crucial for achieving efficient use of ocean space as the aquaculture industry continues to expand in Chile and beyond.

References

Anderson, R. M., and R. M. May. 1979. Population biology of infectious diseases: Part I. *Nature* 280:361–367. doi:10.1038/280361a0.

Asche, F., and T. Bjorndal. 2011. Investment in a salmon farm. In *The economics of salmon aquaculture*, 2nd ed., ed. K. Heen, 201–219. Oxford, UK: Wiley-Blackwell.

Azavedo, D. J. S., J. E. L. Barbosa, W. I. A. Gomes, D. E. Proto, J. C. Marques, and J. Molozzi. 2015. Diversity measures in macroinvertebrate and zooplankton communities related to the trophic status of subtropical reservoirs: Contradictory or complementary responses? *Ecological Indicators* 50:135–149. doi:10.1016/j.ecolind.2014.10.010.

Barrett, G., M. I. Caniggia, and L. Read. 2002. "There are more vets than doctors in Chiloé": Social and community impact of the globalization of aquaculture in Chile. *World Development* 30:1951–1965. doi:10.1016/S0305-750X(02)00112-2.

Barton, J. R. 1997. Environment, sustainability and regulation in commercial aquaculture: The case of Chilean salmonid production. *Geoforum* 28:313–328. doi:10.1016/S0016-7185(97)00013-4.

Barton J., and A. Fløysand. 2010. The political ecology of Chilean salmon aquaculture, 1982–2010: A trajectory from economic development to global sustainability. *Global Environmental Change* 20:739–752. doi: 10.1016/j.gloenvcha.2010.04.001.

Battista, W., J. Ellis, K. Jacobsen, L. Kaplan, J. Price, M. Villarreal, and C. Costello. 2012. *Bioeconomic modeling of salmon farming practices in Southern Chile*. Santa Barbara, CA: University of California.

Black, K., P. K. Hansen, and M. Holmer. 2008. *Salmon Aquaculture Dialogue: Working group report on benthic impacts and farm siting*. WWF.

Burridge, L., J. S. Weis, F. Cabello, J. Pizarro, and K. Bostick. 2010. Chemical use in salmon aquaculture: A review of current practices and possible environmental effects. *Aquaculture* 306:7–23. doi:10.1016/j.aquaculture.2010.05.020.

Buschmann, A. H., F. Cabello, K. Young, J. Carvajal, D. A. Varela, and L. Henríquez. 2009. Salmon aquaculture and coastal ecosystem health in Chile: Analysis of regulations, environmental impacts and bioremediation systems. *Ocean & Coastal Management* 52:243–249. doi:10.1016/j.ocecoaman.2009.03.002.

Buschmann, A. H., D. A. López, and A. Medina. 1996. A review of the environmental effects and alternative production strategies of marine aquaculture in Chile. *Aquacultural Engineering* 15:397–421. doi:10.1016/S0144-8609(96)01006-0.

Buschmann, A. H., V. A. Riquelme, M. C. Hernández-González, D. Varela, J. E. Jiménez, L. A. Henríquez, P. A. Vergara, R. Guíñez, and L. Filún. 2006. A review of the impacts of salmonid farming on marine coastal ecosystems in the Southeast Pacific. *ICES Journal of Marine Science: Journal du Conseil* 63:1338–1345. doi:10.1016/j.icesjms.2006.04.021.

Cacho, O. J. 1997. Systems modelling and bioeconomic modelling in aquaculture. *Aquaculture Economics & Management* 1:45–64. doi:10.1080/13657309709380202.

Chen, Y. S., M. C. M. Beveridge, T. C. Telfer, and W. J. Roy. 2003. Nutrient leaching and settling rate characteristics of the faeces of Atlantic salmon (*Salmo salar* L.) and the implications for modelling of solid waste dispersion. *Energy* 19:114–117.

Farías, L. 2003. Remineralization and accumulation of organic carbon and nitrogen in marine sediments of eutrophic bays: The case of the Bay of Concepción, Chile. *Estuarine, Coastal and Shelf Science* 57:829–841. doi:10.1016/S0272-7714(02)00414-6.

Fløysand, A., H. Avard Haarstad, and J. Barton. 2010. Global economic imperatives, crisis generation and local spaces of engagement in the Chilean aquaculture industry. *Norsk Geografisk Tidsskrift—Norwegian Journal of Geography* 64:199–210. doi:10.1080/00291951.2010.528226.

Forster, J. 1995. Salmon aquaculture: Meeting the value expectations of a mass market. In *Culture of high-value fishes in Asia and the United States*, ed. K. L. Main and C. Rosenfelds, 209–218. Honolulu, HI: Oceanic Institute.

Gao, Q.-F., K.-L. Cheung, S.-G. Cheung, and P. K. S. Shin. 2005. Effects of nutrient enrichment derived from fish farming activities on macroinvertebrate assemblages in a subtropical region of Hong Kong. *Marine Pollution Bulletin* 51:994–1002. doi:10.1016/j.marpolbul.2005.01.009.

Guttormsen, A. G. 2008. Faustmann in the sea: Optimal rotation in aquaculture. *Life Sciences* 23:401–410.

Guy, D. R., S. C. Bishop, S. Brotherstone, A. Hamilton, R. J. Roberts, B. J. McAndrew, and J. A. Woolliams. 2006. Analysis of the incidence of infectious pancreatic necrosis mortality in pedigreed Atlantic salmon, *Salmo salar* L., populations. *Journal of Fish Diseases* 29:637–647. doi:10.1111/jfd.2006.29.issue-11.

Heuch, P. A., and T. A. Mo. 2001. A model of salmon louse production in Norway: Effects of increasing salmon production and public management measures. *Diseases of Aquatic Organisms* 45:145–152. doi:10.3354/dao045145.

Hnath, J. G. 2002. Infectious pancreatic necrosis. In *A guide to integrated fish health management in the Great Lakes Basin*, ed. F. P. Meyer, J. W. Warren, and T. G. Carey, 169. Ann Arbor, MI: Great Lakes Fishery Commission.

Howarth, R. W. 1988. Nutrient limitation of net primary production in marine ecosystems. *Annual Review of Ecology and Systematics* 19:89–110. doi:10.1146/annurev.es.19.110188.000513.

Hvalpsund Net. 2011. *Fishfarming equipment*. Farsø, Denmark: Hvalpsund Net.

Ibieta, P., V. Tapia, C. Venegas, M. Hausdorf, and H. Takle. 2011. Chilean salmon farming on the horizon of sustainability: Review of the development of a highly intensive production, the ISA crisis and implemented actions to reconstruct a more sustainable aquaculture industry. In *Aquaculture and the Environment—A Shared Destiny*, ed. B. Sladonja, 227. InTech. Retrieved from http://www.intechopen.com/books/aquaculture-and-the-environment-a-shared-destiny/chilean-salmon-farming-on-the-horizon-of-sustainability-review-of-the-development-of-a-highly-intens

Jensen, Ø., T. Dempster, E. B. B. Thorstad, I. Uglem, and A. Fredheim. 2010. Escapes of fishes from Norwegian sea-cage aquaculture : Causes, consequences and prevention. *Aquaculture Environment Interactions* 1:71–83. doi:10.3354/aei00008.

Krkosek, M., A. Bateman, S. Proboszcz, and C. Orr. 2010. Dynamics of outbreak and control of salmon lice on two salmon farms in the Broughton Archipelago, British Columbia. *Aquaculture Environment Interactions* 1(2): 137–146. doi:10.3354/aei00014.

Marine Harvest. 2010. *Salmon farming industry handbook 2010*, 68. *Atlantic*. Norway: Marine Harvest. Retrieved from http://www.marineharvest.com/globalassets/investors/handbook/2015-salmon-industry-handbook.pdf

Mayor, D. J., M. Solan, I. Martínez, L. Murray, H. McMillan, G. I. Paton, and K. Killham. 2008. Acute toxicity of some treatments commonly used by the salmonid aquaculture industry to *Corophium volutator* and *Hediste diversicolor*: Whole sediment bioassay tests. *Aquaculture* 285:102–108. doi:10.1016/j.aquaculture.2008.08.008.

McAllister, P. 1983. *Infectious pancreatic necrosis (IPN) of salmonid fishes*. US Fish & Wildlife Publications. http://digitalcommons.unl.edu/usfwspubs/141.

Mccausland, W. D., E. Mente, G. J. Pierce, and I. Theodossiou. 2006. A simulation model of sustainability of coastal communities : Aquaculture, fishing, environment and labour markets. *Ecological Modelling* 193:271–294. doi:10.1016/j.ecolmodel.2005.08.028.

Montiel, A., E. Quiroga, and D. Gerdes. 2011. Diversity and spatial distribution patterns of polychaete assemblages in the Paso Ancho, Straits of Magellan Chile. *Continental Shelf Research* 31:304–314. doi:10.1016/j.csr.2010.11.010.

Nash, C., P. Brubridge, and J. Volkman. 2005. Guidelines for ecological risk assessment of marine fish aquaculture. NOAA Technical Memorandum NMFS-NWFSC-71. http://www.aces.edu/dept/fisheries/education/documents/MarineAquacultureRiskAssessmentGuidelines.pdf.

Naylor, R., K. Hindar, I. A. Fleming, R. Goldburg, S. Williams, J. Volpe, F. Whoriskey, J. Eagle, D. Kelso, and M. Mangel. 2005. Fugitive salmon: Assessing the risks of escaped fish from net-pen aquaculture. *BioScience* 55:427–437. doi:10.1641/0006-3568(2005)055[0427:FSATRO]2.0.CO;2.

Nobre, A. M., J. K. Musango, M. P. De Wit, and J. G. Ferreira. 2009. A dynamic ecological–economic modeling approach for aquaculture management. *Ecological Economics* 68:3007–3017. doi:10.1016/j.ecolecon.2009.06.019.

Ocean Conservancy. 2011. *Right from the start: Open-ocean aquaculture in the United States*. Washington, DC: Ocean Conservancy.

Pitchon, A. 2011. Sea hunters or sea farmers? Transitions in Chilean fisheries. *Human Organization* 70:200–209. doi:10.17730/humo.70.2.q66v20403172hh3t.

Polasky, S., E. Nelson, J. Camm, B. Csuti, P. Fackler, E. Lonsdorf, C. Montgomery, D. White, J. Arthur, B. Garber-Yonts, R. Haight, J. Kagan, A. Starfield, and C. Tobalske. 2008. Where to put things? Spatial land management to sustain biodiversity and economic returns. *Biological Conservation* 141:1505–1524. doi:10.1016/j.biocon.2008.03.022.

Pomeroy, R., B. E. Bravo-Ureta, D. Solís, and R. J. Johnston. 2008. Bioeconomic modelling and salmon aquaculture: An overview of the literature. *International Journal of Environment and Pollution* 33:485–500. doi:10.1504/IJEP.2008.020574.

Rabalais, N. N. 2002. Nitrogen in aquatic ecosystems. *AMBIO: A Journal of the Human Environment* 31(2): 102–112. doi:10.1579/0044-7447-31.2.102.

Scheel, I., M. Aldrin, A. Frigessi, and P. A. Jansen. 2007. A stochastic model for Infectious Salmon Anemia (ISA) in Atlantic salmon farming. *Journal of the Royal Society* 4:699–706.

Shannon, C. 1948. A mathematical theory of communication. *Bell System Technical Journal* 27(4): 623–656. doi:10.1002/bltj.1948.27.issue-4.

Silvert, W., and J. W. Sowles. 1996. Modelling environmental impacts of marine finfish aquaculture. *Journal of Applied Ichthyology* 12:75–81. doi:10.1111/jai.1996.12.issue-2.

Sistema de Autentificación Centralizada, Activites Outstanding Profile and Process (SEIA). Servicio de Evaluación Ambiental. Retrieved from http://seia.sea.gob.cl/actividades/actividadesPorPerfil.php (accessed 14 February 2012).

Soares, S., D. M. Green, J. F. Turnbull, M. Crumlish, and A. G. Murray. 2011. A baseline method for benchmarking mortality losses in Atlantic salmon (*Salmo salar*) production. *Aquaculture* 314:7–12. doi:10.1016/j.aquaculture.2011.01.029.

Soto, D., I. Arismendi, J. González, J. Sanzana, F. Jara, C. Jara, E. Guzmán, and A. Lara. 2006. Southern Chile, trout and salmon country: Invasion patterns and threats for native species. *Revista Chilena de Historia Natural* 79:97–117. doi:10.4067/S0716-078X2006000100009.

Soto, D., F. Jara, and C. Moreno. 2001. Escaped salmon in the inner seas, southern Chile: Facing ecological and social conflicts. *Ecological Applications* 11:1750–1762. doi:10.1890/1051-0761(2001)011[1750:ESITIS]2.0.CO;2.

Sylvia, G., J. L. Anderson, and D. Cai. 1996. A multilevel, multiobjective policy model: The case of marine aquaculture development. *American Journal of Agricultural Economics* 78:79–88. doi:10.2307/1243780.

Tironi, A., V. H. Marin, and F. J. Campuzano. 2010. A management tool for assessing aquaculture environmental impacts in Chilean Patagonian fjords: Integrating hydrodynamic and pellets dispersion models. *Environmental Management* 45:953–962. doi:10.1007/s00267-010-9467-5.

Veldhoen, N., M. G. Ikonomou, C. Buday, J. Jordan, V. Rehaume, M. Cabecinha, C. Dubetz, J. Chamberlain, S. Pittroff, K. Vallée, G. Van Aggelen, and C. C. Helbing. 2012. Biological effects of the anti-parasitic chemotherapeutant emamectin benzoate on a non-target crustacean, the spot prawn (*Pandalus platyceros* Brandt, 1851) under laboratory conditions. *Aquatic Toxicology* 108:94–105. doi:10.1016/j.aquatox.2011.10.015.

Watershed Watch. 2001, December. *Salmon farms, sea lice, & wild salmon: A watershed watch report on risk, responsibility, and the public interest*. Report. Coquitlam, British Columbia: Watershed Watch Salmon Society. Retrieved from https://www.watershed-watch.org/publications/files/WWSS_Sea_Lice_Report.pdf

White, C., B. S. Halpern, and C. V. Kappel. 2012. Ecosystem service tradeoff analysis reveals the value of marine spatial planning for multiple ocean uses. *Proceedings of the National Academy of Sciences* 109:4696–4701.

World Wildlife Federation (WWF). 2009. *Salmon escapes in Chile: Incidents, impacts, mitigation, and prevention*. Chile: World Wildlife Federation.

Appendix

Technology classes

Technology Class 1 represents conditions commonly found early in the emergence of the salmon aquaculture industry in Chile (1980s), and corresponds with reported escapes of 30% per cycle (Naylor et al. 2005; Molina, pers. comm., 2012). During this period, nets were commonly made of weak or damaged material discarded from fishing vessels, and pens were moored to the sea floor at only two places, making them vulnerable to capsizing in strong currents or during severe weather conditions (see Figure A1). Additionally, during this period no scientific assessment was carried out to determine the best placement of the pens, and there was little to no staff training on the best management techniques to prevent escapes.

Technology Class 2 represents conditions at the start of industry expansion (early 1990s) when new nets were purchased, predator prevention nets were installed, and pens were moored in a grid pattern to prevent capsizing (see Figure A2). This period also saw the start of scientific analysis to determine ideal placement based on current speed and depth of the seafloor, as well as an increase in staff trainings with the goal of improving management techniques to reduce escapes. This class corresponds with 20% escapes per cycle (Naylor et al. 2005; Molina, pers. comm., 2012).

Technology Class 3 represents what is currently the most widely available aquaculture net pen and mooring technology, which includes stronger net materials such as Kevlar and polyethylene as

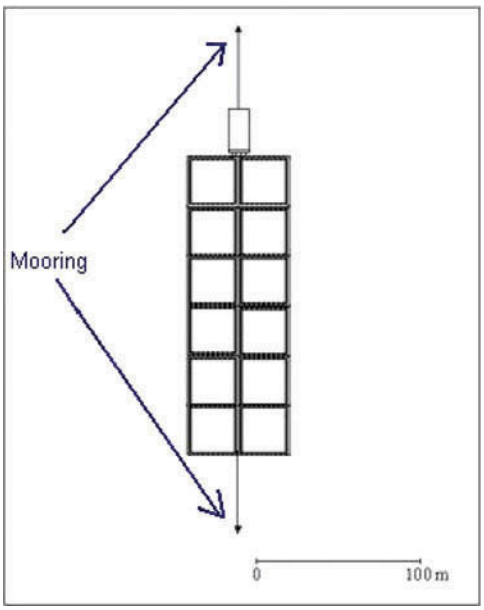

Figure A1. Technology Class 1 farm diagram, moored at only two points.

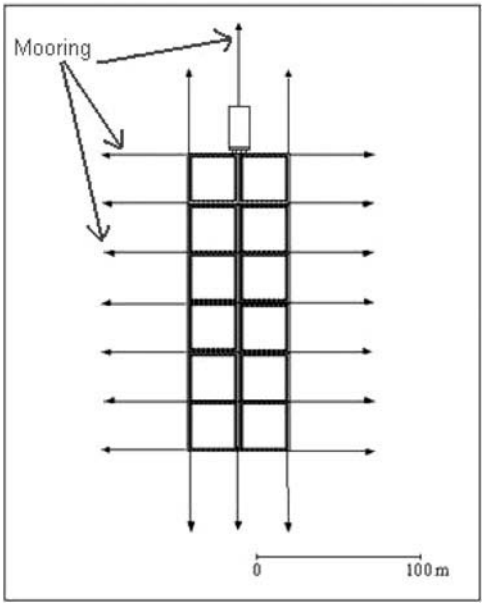

Figure A2. Technology Class 2 and 3 farm diagram, moored in a grid pattern.

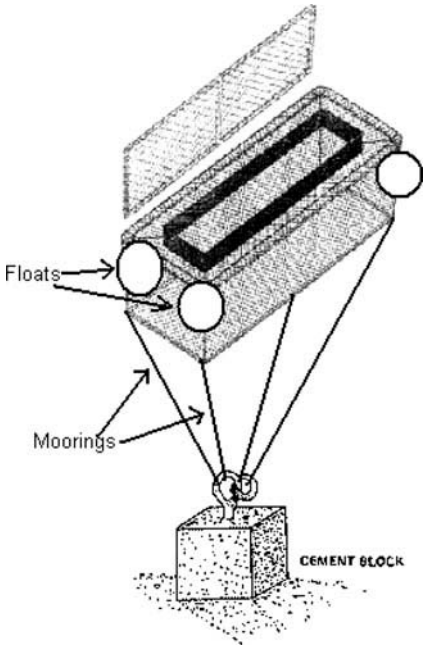

Figure A3. Technology Class 4 diagram, solid copper cage.

well as antifouling paints to reduce maintenance needs (Hvalpsund Net 2011). Science on the design and placement of net pens has also improved, and staff training requirements have increased. This class corresponds with approximately 5% escapes per cycle (Naylor et al. 2005; Jensen, pers. comm., 2012; Molina, pers. comm., 2012).

Technology Class 4 represents a potential next step in large-scale salmon aquaculture—the use of solid copper cages in place of net pens (see Figure A3). This technology is impervious to rips and predators and extremely resistant to capsizing and therefore hypothetically corresponds with 0% escapes per cycle (Molina, pers. comm., 2012). While our four classes are loosely associated with successive periods over the evolution of the industry, it is feasible that any of the four classes might be found at a given concession in Chile today.

Predation competition equations

In order to model the predator/prey interactions of the escaped salmon with the wild Chilean species, we utilized the basic Lotka-Volterra predator/prey equations (amended to account for density dependent growth):

$$\frac{dx}{dt} = x(\vartheta - \varphi y - \psi x - \varphi' z). \tag{A1}$$

and

$$\frac{dy}{dt} = y(\Delta x - \Sigma - \zeta y). \tag{A2}$$

We assigned each variable with the following meanings:
y = number of some predator species (e.g., hake);
x = number of the predator's prey species (e.g., sardines);
ϑ = intrinsic growth rate of the prey species;
φ = rate of predation on prey by native predators;
ψ = density-dependent growth dampener for prey (negative growth rate);
φ' = rate of predation on prey by escaped salmon;
z = number of escaped salmon time zero;
t = time in months;
Δ = conversion efficiency between prey and predators (i.e., how much the presence of prey "helps" predators);
Σ = intrinsic mortality rate of the predator species; and
ζ = density-dependent growth dampener for predators (negative growth rate).

This model does not include the more complicated interactions between more than two species. Additionally, the Lotka-Volterra model depends on a number of assumptions, including: The food supply of the predator population depends entirely on the prey population; the rate of change of a population is proportional to its size; the environment does not change; and genetic adaptation is inconsequential.

We manipulated these equations algebraically to determine the system at equilibrium (no change in x or y):

$$\vartheta - \varphi y - \psi x - \varphi' z = 0. \tag{A3}$$

$$y = (\vartheta - \psi x - \vartheta' z)/\vartheta. \tag{A4}$$

and

$$\Delta x - \Sigma - \zeta y = 0. \tag{A5}$$

$$y = (\Delta x - \Sigma)/\zeta. \tag{A6}$$

set equal:

$$(\vartheta - \psi x - \vartheta' z)/\vartheta = (\Delta x - \Sigma)/\zeta. \tag{A7}$$

$$\vartheta - \psi x - \varphi' z = \frac{\varphi \Delta x - \varphi \Sigma}{\zeta}. \tag{A8}$$

$$\vartheta - \psi x - \varphi' z + \left(\frac{\varphi \Sigma}{\zeta}\right) = \frac{\varphi \Delta x}{\zeta}. \tag{A9}$$

$$\vartheta - \varphi' z + \left(\frac{\varphi \Sigma}{\zeta}\right) = x\left(\left(\frac{\varphi \Delta}{\zeta}\right) + \psi\right). \tag{A10}$$

$$x = \frac{\vartheta - \varphi' z + \left(\frac{\varphi \Sigma}{\zeta}\right)}{\left(\frac{\varphi \Delta}{\zeta}\right) + \psi}. \tag{A11}$$

plug in for y:

$$y = \frac{\Delta\left(\frac{\left(\vartheta - \varphi' z + \left(\frac{\varphi \Sigma}{\zeta}\right)\right)}{\left(\left(\frac{\varphi \Delta}{\zeta}\right) + \psi\right)}\right) - \Sigma}{\zeta}. \tag{A12}$$

We solved for fractional changes in the number of native predator and prey individuals after the addition of the escaped salmon escapes (with the system at steady state). Through these manipulations we determined that:

$$\frac{x(\textit{with escapes})}{x(\textit{without escapes})} = \left(\frac{\vartheta - \varphi' z + \left(\frac{\varphi \Sigma}{\zeta}\right)}{\left(\frac{\varphi \Delta}{\zeta}\right) + \psi}\right) \times \left(\frac{\left(\frac{\varphi \Delta}{\zeta}\right) + \psi}{\vartheta + \left(\frac{\varphi \Sigma}{\zeta}\right)}\right). \tag{A13}$$

$$\frac{x(\textit{with escapes})}{x(\textit{without escapes})} = \left(\frac{\vartheta - \varphi' z + \left(\frac{\varphi \Sigma}{\zeta}\right)}{\vartheta + \left(\frac{\varphi \Sigma}{\zeta}\right)}\right), \tag{A14}$$

which simplifies to:

$$\frac{x(\textit{with escapes})}{x(\textit{without escapes})} = 1 - \left(\frac{\varphi' z}{\vartheta + \left(\frac{\varphi \Sigma}{\zeta}\right)}\right), \tag{A15}$$

which is linear.

To solve for fractional change in number of predator individuals after addition of escapes (with system at steady state):

$$\frac{y(\textit{with escapes})}{y(\textit{without escapes})} = \left(\frac{\Delta\left(\frac{\left(\vartheta - \varphi' z + \left(\frac{\varphi \Sigma}{\zeta}\right)\right)}{\left(\left(\frac{\varphi \Delta}{\zeta}\right) + \psi\right)}\right) - \Sigma}{\zeta}\right) \times \left(\frac{\zeta}{\Delta\left(\frac{\left(\vartheta + \left(\frac{\varphi \Sigma}{\zeta}\right)\right)}{\left(\left(\frac{\varphi \Delta}{\zeta}\right) + \psi\right)}\right) - \Sigma}\right). \tag{A16}$$

$$\frac{y(\textit{with escapes})}{y(\textit{without escapes})} = \frac{\Delta\left(\frac{\left(\vartheta - \varphi' z + \left(\frac{\varphi \Sigma}{\zeta}\right)\right)}{\left(\left(\frac{\varphi \Delta}{\zeta}\right) + \psi\right)}\right) - \Sigma}{\Delta\left(\frac{\left(\vartheta + \left(\frac{\varphi \Sigma}{\zeta}\right)\right)}{\left(\left(\frac{\varphi \Delta}{\zeta}\right) + \psi\right)}\right) - \Sigma}, \tag{A17}$$

which simplifies to:

$$\frac{y(with\ escapes)}{y(without\ escapes)} = \frac{\left(\frac{\vartheta\Delta}{\left(\left(\frac{\varphi\Delta}{\zeta}\right)+\psi\right)}\right) - \left(\frac{\varphi' z\Delta}{\left(\left(\frac{\varphi\Delta}{\zeta}\right)+\psi\right)}\right) + \left(\frac{\frac{\varphi\Sigma\Delta}{\zeta}}{\left(\left(\frac{\varphi\Delta}{\zeta}\right)+\psi\right)}\right) - \Sigma}{\left(\frac{\vartheta\Delta}{\left(\left(\frac{\varphi\Delta}{\zeta}\right)+\psi\right)}\right) + \left(\frac{\frac{\varphi\Sigma\Delta}{\zeta}}{\left(\left(\frac{\varphi\Delta}{\zeta}\right)+\psi\right)}\right) - \Sigma}. \tag{A18}$$

$$\frac{y(with\ escapes)}{y(without\ escapes)} = 1 - z\frac{\frac{\varphi'\Delta}{\left(\left(\frac{\varphi\Delta}{\zeta}\right)+\psi\right)}}{\left(\Delta\left(\frac{\vartheta+\left(\frac{\varphi\Sigma}{\zeta}\right)}{\left(\left(\frac{\varphi\Delta}{\zeta}\right)+\psi\right)}\right)\right) - \Sigma}, \tag{A19}$$

which is also linear.

Because these relationships are linear, and we were therefore able to identify the number of escaped salmon that would reduce both native populations by a specific percentage and then use those numbers to calculate the fractional change that would be expected in x and y due to the addition of the predicted number of escaped salmon in our modeled cycle. We were thus able to insert the following equations into our model:

$$Fractional\ Change\ Predator = 1 - \left(\left(\frac{0.5}{50,000}\right) \times [predicted\ \#\ escapes]\right). \tag{A20}$$

$$Fractional\ Change\ Prey = 1 - \left(\left(\frac{0.5}{50,000}\right) \times [predicted\ \#\ escapes]\right) \tag{A21}$$

and

$$Fractional\ Change\ Cetaceans = 1 - \left(\left(\frac{0.5}{50,000}\right) \times [predicted\ \#\ escapes]\right) \tag{A22}$$

Spread of disease and sea lice equations

Spread of disease *within* pens to other salmon:

$$\frac{d\mathrm{H}}{dt} = \Theta - \mathrm{HM} - \mu\mathrm{H}\sigma - \mathrm{H}\varepsilon \tag{A23}$$

for change in healthy salmon, and

$$\frac{d\sigma}{dt} = \mu\mathrm{H}\sigma - (\sigma(\mathrm{M} + u)) - \sigma\varepsilon \tag{A24}$$

for change in sick salmon. In these equations,

H = number of healthy salmon;

σ = number of sick salmon;

t = time in months;

Θ = population growth of healthy salmon (0 because they do not reproduce);

M = natural mortality rate for the healthy salmon;

u = mortality rate from disease;

μ= disease transmission coefficient within pens; and

ε = percent of salmon that escape in one cycle based on the technology class.

The spread of sea lice was modeled using essentially the same methods that were used for the spread of disease, with the following adjustments: The equations were amended to allow for salmon to contract sea lice from the native species as well as transmit sea lice to the native

species (because sea lice is likely already present in the native ecosystem before aquaculture is introduced); species mortality rates due to sea lice were assumed to be much lower than for the IPN virus because adult salmon can survive even with relatively large numbers of lice; and the transmission coefficient for sea lice was assumed to be much higher than for IPN because low levels of sea lice are quite common throughout aquaculture industries worldwide (Watershed Watch 2001). We chose to model the spread of IPN instead of ISA because testing for the ISA virus is performed on a regular basis, and if it is detected all salmon in the farm are immediately exterminated and removed (Marine Harvest 2010; Scheel et al. 2007).

Spread of sea lice *within* pens to other salmon:

$$\frac{d\mathrm{H}}{dt} = \Theta - \mathrm{HM} - \mu\mathrm{H}(\sigma + Q) - \mathrm{H}\varepsilon \tag{A25}$$

for change in sea lice-infested salmon, and

$$\frac{d\sigma}{dt} = \mu\mathrm{H}(\sigma + Q) - (\sigma(\mathrm{M} + \nu)) - \sigma\varepsilon \tag{A26}$$

for change in sick salmon. In these equations, Q = number of sick or infested native animals.

Spread of disease or sea lice *outside* of pens to native populations:

$$\frac{d\mathrm{H}}{dt} = \Theta - \mathrm{HM} - \mu\mathrm{H}(\sigma + \mathrm{Z}) \tag{A27}$$

for change in healthy animals, and

$$\frac{d\mu}{dt} = \mu\mathrm{H}(\sigma + \mathrm{Z}) - (\sigma(\mathrm{M} + u)) \tag{A28}$$

for change in sick (or infested) animals. In these equations, Z is calculated by multiplying the number of sick (or infested) salmon in a concession by the percent that escape, as determined by the Technology Class in use.

We assumed that 5% of incoming smolt are infected with the IPN, but only 10 individual smolt are infected with sea lice (based on studies showing that salmon smolt enter the pens relatively free of lice) (Heuch and Mo 2001; Krkosek et al. 2010).

Baseline values for native species are not known for southern Chile, so placeholder values were used that would be sufficiently large to allow for the model to run throughout the length of a cycle. New healthy individuals in time 2 is calculated as healthy individuals in time 1 plus change in healthy individuals. New sick/infested individuals in time 2 is calculated as sick/infested individuals in time 1 plus change in sick/infested individuals. These calculations were done on a month-to-month basis for the number of months equal to the length of the cycle. Then, fractional changes were calculated as follows:

$$\textit{Fractional Change in Healthy Individuals} = \frac{H_{cycle}}{H_{t-1}} \tag{A29}$$

where H_{cycle} = the number of healthy individuals in the month corresponding with the last month of the cycle, and $H_{t=1}$ = the number of healthy individuals at the start of the cycle. This process was repeated for the three trophic levels: predators, prey, and cetaceans.

Feed, SLICE, and labor cost calculations

We calculated the cost of feed with the following equation:

$$f(t) = \gimel \times Y \times T \tag{A30}$$

where ϡ = cost of feed per kg, Y = the economic feed conversion ratio, and T = the total harvest weight in kg.

We used the cost of SLICE to calculate the cost of chemicals with the following equation:

$$c(t) = G \times \rho \times A \times \bar{w} \times J \times ß. \tag{A31}$$

where G = cost of SLICE per kg, Þ = dose per fish, A = average number of fish, $\bar{w}$ = average weight of fish, J = 7 days of treatment, and $ß$ = the number of treatments per cycle (which is also a model input).

We calculated the cost of labor with the following equation:

$$i(t) = W \times X \times \overset{\circ}{a}\, \omega. \tag{A32}$$

where Ш = minimum wage per hour, X = maximum allowable work hours per week, å = cycle length in weeks, and ϡ = the average number of workers at a farm.

Tables A1. Maintenance costs by technology class.

Class	Tightening moorings	Cleaning/repairing/ replacing nets	Staff training (at hourly worker wage)
1	US$2,000 per net pen, twice per cycle (based on diver wages)	US$400 per net pen, twice per month	0 hours per cycle
2	US$6,000 per net pen, twice per cycle	US$400 per net pen, twice per month	10 hours per cycle
3	US$6,000 per net pen, twice per cycle	US$400 per net pen, once per month (less need due to antifoulant paints and stronger materials)	20 hours per cycle
4	US$2,000 per cage, once per month (due to the configuration of these cages, moorings can be tightened in less time)	N/A (Completed by diver who tightens moorings)	40 hours per cycle

Table A2. ISA transmission submodel assumptions.

Assumption	Justification
Detection of the ISA virus takes 7 months from initial infection.	The true detection time ranges between 6 and 9 months (Scheel et al. 2007); however, because salmon facilities in Chile test their farmed salmon for disease frequently (per government regulation), we assumed detection will occur at the low end of the range.
The monthly probability of detection equals 0.163 and the monthly probability of detection is the inverse, 0.837.	1=(p+p(1−p)+ p(1−p)^2+ p(1−p)^3+ p(1−p)^4+ p (1−p)^5+ p(1−p)^6)
The baseline probability of infection each month (i.e., from infected smolt) is 0.0008. The inverse of this probability, which represents the probability that an uninfected farm will remain uninfected, is 0.9992.	Scheel et al. (2007)
The probability of a farm shifting from Infected/ Detected to uninfected is always 1 because all salmon in the infected farm will be slaughtered when ISA is detected.	Carlos Odebret, Salmon Chile, pers. comm.
$k_{ji} = 1$ as a network indicator	Assumes farms modeled are within the same concession.
$l_{ji} = 1$ as a transmission indicator	Of the farms modeled, one is infected and the other is susceptible to ISA.
$d(x_j,x_i)_{=5}$	Data were unavailable for distance between individual farms; determined based on expert knowledge.

Table A3. Parameter values and assumptions.

Submodel	Parameter	Symbol	Value used	Source and assumptions
Nutrients	Percent of feed excreted in salmon feces	E	0.15	Black et al. (2008)
	Percent of feed eaten by salmon	F	0.97	Average from EIAs
	Percent N content of salmon feed by weight	U_{feed}	6.24 g/kg feed	Black et al. (2008)
	Economic food conversion ratio	Y	1.25	Average from EIAs
	Tonnes of salmon production expected from one form during one harvest cycle	K	Calculated in Harvest Revenue submodel.	Estimated the number of farms in each concession based on the number of net pens, assuming that there are eight net pens per farm
	Percent N content of salmon feed by weight	U_{feces}	0.065	Barton (1997)
	Current speed	W	Obtained individually from EIAs.	EIAs
	Water depth	D	Obtained individually from EIAs.	EIAs
	Settling speed of salmon feces	s_{feces}	4 cm/sec	Average from Chen et al. (2003) and Tironi et al. (2010)
	Settling speed of salmon feed	s_{feed}	11 cm/sec	Tironi et al. (2010)
Chemicals	Slice dosage	Ψ	50 ug/kg fish biomass × 7 days	SLICE Recommended Dose by Merck Animal Health
	Leaching rate		50 ug/cm2/day	Authors' estimate
	Number of days in a month	κ	30 days/month	
	Surface area of the outside of a box representing a rectangular net	ς	6,400 m2	Assumed the box is 40 × 40 × 20 m
	Area of the top of a box representing a rectangular net	ϱ	1,600 m2	40 × 40 m
	Fraction of a box that is actually a painted surface	υ	0.1	Authors' estimate; would vary depending on mesh size and net material

(*Continued*)

Table A3. (Continued).

Submodel	Parameter	Symbol	Value used	Source and assumptions
Escapes—Disease Transmission	Number of healthy native predators at start	H	100,000	Arbitrary number; fractional change measured
	Number of healthy native prey at start	H	1,000,000	Arbitrary number, fractional change measured
	Number of healthy cetaceans at start	H	1,000	Arbitrary number; fractional change measured
	Number of healthy salmon at start	H	Obtained individually from EIAs	Number of starting salmon from EIAs; number of sick salmon at start (s) calculated as below
	Number of sick native predators at start	Q	200	Arbitrary number; fractional change measured
	Number of sick native prey at start	Q	2,000	Arbitrary number; fractional change measured
	Number of sick cetaceans at start	Q	20 for sea lice; 0 for disease	Arbitrary number; fractional change measured
	Number of sick salmon at start	Q	Starting Number of Smolt * 0.05	Assumed 5% of salmon arrive with IPN based on Guy et al. (2006)
	Time (months)	t	length of cycle (12–18)	EIAs
	Population growth rate of healthy predators	Θ	0.0108	Authors' estimate
	Population growth rate of healthy prey	Θ	0.032	Authors' estimate
	Population growth rate of healthy cetaceans	Θ	0.00417	James Harvey, Moss Landing Marine Labs, pers. comm.
	Natural mortality rate of healthy predators	M	0.0125	Authors' estimate
	Natural mortality rate of healthy prey	M	0.03	Authors' estimate
	Natural mortality rate of healthy cetaceans	M	0.00583	James Harvey, Moss Landing Marine Labs, pers. comm.
	Natural mortality rate of salmon	M	0.005	Asche and Bjorndal (2011)
	Disease transmission coefficient—within pens	μ	0.00000026	Authors' estimate
	Disease transmission coefficient—outside pens	μ	0.00000026	Authors' estimate
	Sea lice transmission coefficient	μ	0.00000231	Authors' estimate
	Sea lice transmission coefficient	μ	0.00000231	Authors' estimate
	Mortality due to disease	u	0.0017857	Varied from 2% per cycle to 50% per cycle, based on Guy et al. 2006
	Mortality due to sea lice	u	0.0000007	Authors' estimate
	Number of sick salmon escapes	Z	Calculated as p*Starting Number of Smolt	Starting number of salmon from EIAs; percent of fish lost (p) calculated as below
	Percent of fish lost based on result of Technology Class	ε	100% if Q = 0, 30% if Q = 1, 20% if Q = 2, 5% if Q = 3, 0% if Q = 4	Naylor et al. (2005); Molina, pers. comm., (2012); Jensen, pers. comm., (2012)

(*Continued*)

Table A3. (Continued).

Submodel	Parameter	Symbol	Value used	Source and assumptions
Escapes—Competition/Predation	Number of escapes required to reduce native predator population by half	No symbol	50,000	Arbitrary number; fractional change measured
	Number of escapes required to reduce native prey population by half	No symbol	50,000	Arbitrary number; fractional change measured
	Number of escapes required to reduce native cetation population by half	No symbol	100,000	Arbitrary number; fractional change measured
	Number of some predator species (e.g., hake)	y	No value needed for calculation	
	Number of the predator's prey species (e.g., sardines)	x	No value needed for calculation	
	Intrinsic growth rate of the prey species	ϑ	No value needed for calculation	
	Rate of predation on prey by native predators	φ	No value needed for calculation	
	Density-dependent growth dampener for prey (negative growth rate)	ψ	No value needed for calculation	
	Rate of predation on prey by escaped salmon	φ'	No value needed for calculation	
	Number of escaped salmon time zero	z	No value needed for calculation	
	Time in months	t	No value needed for calculation	
	Conversion efficiency between prey and predators (i.e., how much the presence of prey "helps" predators)	Δ	No value needed for calculation	
	Intrinsic mortality rate of the predator species	Σ	No value needed for calculation	
	Density-dependent growth dampener for predators (negative growth rate)	ζ	No value needed for calculation	

(*Continued*)

Table A3. (Continued).

Submodel	Parameter	Symbol	Value used	Source and assumptions
Risk Cost of ISA	Network indicator (1 if both farms are in the same concession, 0 otherwise)	k_{ji}	1	Our model only looks at two farms within the same concession.
	Transmission indicator (1 if one farm is infected and the other is susceptible, 0 otherwise)	I_{ji}	1	Our model only looks at this scenario.
	Number of months into the cycle at which detection of the outbreak occurs	δ	7	Scheel et al. (2007) estimated it takes 6–9 months to detect ISA; we assumed detection would occur in month 7
	Biomass/transmission coefficient	α	0.127 $(100\ \text{tons})^{-1}$	Scheel et al. (2007)
	Biomass/susceptibility coefficient	β_1	0.102 $(100\ \text{tons})^{-2}$	Scheel et al. (2007)
	Farm spacing/transmission coefficient	ϕ	0.415 km^{-1}	Scheel et al. (2007)
	Network/transmission coefficient	γ	−2.013 (no unit)	Scheel et al. (2007)
Risk Cost of Violations	Number of wage violations	j	3	Average fines per year for the company with the greatest number of fines
	Average fine amount in US$ issued by the Chilean government for individual wage-based labor violations	ξ	2,573.189744	Average was calculated from fines complied from a public database of labor violation records obtained from the Chilean Ministry of Labor's labor inspection website. The labor violation records for 11 salmon aquaculture companies were queried, categorized according to whether the violation was wage-based or hours-based, and then averaged (see SEIA, 2012).
	Number of hours violations	r	2	Average fines per year for the company with the most fines
	Average fine amount in US$ issued by the Chilean government for individual hours-based labor violations	Π	2,304.833662	Average calculated from fines complied from a public database of labor violation records obtained from the Chilean Ministry of Labor's labor inspection website. The labor violation records for 11 salmon aquaculture companies were queried, categorized according to whether the violation was wage-based or hours-based, and then averaged (see SEIA, 2012).
	Probability of detection constant	θ	0.12	Value based on a statistic stating that only 12% of all salmon farming facilities are actually inspected for regulatory compliance (Barton and Fløysand, 2010)

(*Continued*)

Table A3. (Continued).

Submodel	Parameter	Symbol	Value used	Source and assumptions
Aquaculture Revenue and Costs	Weight of salmon at harvest (kg)	w	4.483	calculated with a 14-month cycle
	Time (months)	t	Length of cycle (12–18)	Taken from individual Chilean EIAs
	Biomass in (kg)	b	Dependent on cycle length	Detailed if/then statement
	Price in US$/kg of salmon	p	5.87	Average $/kg for a 14-month cycle (December 2010 to January 2012)
	Cost of feed/kg in US$	ϡ	1.19	Martinez, pers. comm., AVS Chile (converted from pesos: US$1 = 511 Chilean Pesos)
	Economic feed conversion ratio	Y	1.25	Feed conversion ratio of dry feed pellets (average from EIA data)
	Total harvest weight in (kg)	T	4,970,685	calculated
	Cost of smolt	q	0.2	Ibieta et al. (2011)
	Cost of chemicals	c	0.001	Calculated as cost of chemicals/kg Harvestable Salmon
	Cost of SLICE/ per kg in US$	G	120	Personal contact—Sandra Bravo, Universidad Austral de Chile
	Dose of SLICE per fish (µg/kg/day for 7 consecutive days)	Þ	50	http://aqua.merck-animal-health.com/products/slice/information.aspx
	Average number# of fish per cycle	A	1,208,459	Average from EIA data
	Average weight of fish	$\bar{w}$	1.932	Average from EIA data
	Days of treatment	J	7	A week long
	Cost of maintenance	m	190,489.04	calculated
	Cost of labor	l	Varies	calculated as maximum allowable work hours x minimum wage)
	Minimum wage/hr	Ш	1.59	Ministry of Labor of the Chilean Government (http://www.dt.gob.cl/consultas/1613/w3-article-60141.html)
	Maximum allowable work hrs/wk	X	45	Ministry of Labor, Department of Inspection, Chilean Government; International Finance Corporation of the World Bank (http://www.doingbusiness.org/data/exploreeconomies/chile/employing-workers)
	Cycle length (months)	Γ	Length of cycle (12–18)	Minimum and maximum lengths from EIA data
	Cycle length (weeks)	å	Length of cycle (12–18)	Minimum and maximum lengths from EIA data
	Average number# of workers at a farm	Ш	11	Average from EIA data
	Interest and depreciation	i	0.14	Ibieta et al. (2011)
	Other operational costs	o	0.32	Ibieta et al. (2011)
	Costs incurred before salmon are sold on commodity market	a	1.35	38% processing, sales/marketing/transportation
	Cost of an ISA outbreak	L	333	calculated
	Cost of labor violations	v	1,479	calculated
	Total Profit	P	11,548,556	calculated
	Harvest revenue (US$)	R	29,195,671	calculated
	Total cost of harvest	h	17,654,303	Calculated